Supercritical Water Oxidation of a Carbon Particle by Schlieren Photography

Masakazu Sugiyama
Dept. of Electronic Engineering, School of Engineering, The University of Tokyo, Tokyo 113-8656, Japan

Sumiko Tagawa
Dept. of Chemical System Engineering, School of Engineering, The University of Tokyo, Tokyo 113-8656, Japan

Hisao Ohmura
Joint Research Center for Supercritical Fluids, Japan Chemical Innovation Institute, Sendai 983-8551, Japan

Seiichiro Koda
Dept. of Chemistry, Faculty of Science and Technology, Sophia University, Tokyo 102-8554, Japan

DOI 10.1002/aic.10246
Published online in Wiley InterScience (www.interscience.wiley.com).

The flow pattern around a carbon particle (~ 3.5 mm in diameter) during the supercritical water oxidation (SCWO) process (25 MPa, 723 K, 3.6 wt % O_2 concentration) was visualized for the first time by the use of Schlieren optics and a SCWO reactor equipped with transparent sapphire windows. To link Schlieren images with flow fields, computational fluid dynamics (CFD) simulations were executed, assuming temperature-dependent density of supercritical water and heat of a surface reaction, and then the obtained density fields around the particle were numerically converted to Schlieren images. Numerically obtained Schlieren images agreed well with observed images, confirming that the CFD simulation was able to predict the flow field in SCWO processes. Such a combined approach of CFD and flow visualization revealed that, in SCWO of solid substances with a fast reaction rate, the heat of surface reaction increased the temperature of the fluid and induced an upward flow from the particle with higher fluid temperature than that of the surroundings. Such flow can increase reaction rates by enhancing the mass transfer of O_2 to solids. Therefore, a flow field in SCWO is an important factor controlling the progress of reaction and it can be reasonably predicted by CFD simulations. © 2004 American Institute of Chemical Engineers *AIChE J,* 50: 2082–2089, 2004
Keywords: supercritical water oxidation (SCWO), carbon particle, flow pattern, Schlieren image, computational fluid dynamics (CFD)

Introduction

Supercritical fluids technology is now going to be applied in a number of fields (Savage, 1999; Tester et al., 1993). Flow dynamics of a supercritical fluid is of crucial importance with respect to its practical applications using reactions and mass transport. The flow dynamics affects concentration gradients in a reactor and thus influences the uniformity of the reaction rate. In the case of a heterogeneous system consisting of a supercritical fluid and a solid reactant, if a reaction rate is limited by mass transfer, a local velocity field around the solid substantially affects the rate of mass transfer and thus the reaction rate

Correspondence concerning this article should be addressed to S. Koda at s-koda@sophia.ac.jp.

is dependent on the flow pattern. As an example, we observed that the reaction rate of the supercritical water oxidation (SCWO) of an activated carbon particle increased with the flow rate of supplied water (Sugiyama et al., 2002).

Because of their large kinematic viscosity (viscosity/density) and the sensitivity of their density on temperature, supercritical fluids tend to be accompanied by buoyancy-driven flow, which makes it more difficult to predict a flow pattern of a supercritical fluid compared to that of ordinary gases and liquids. Computational fluid dynamics (CFD) simulations have now become a potential tool for analyzing and predicting flow patterns of supercritical fluids (Oh et al., 1995; Zhou et al., 2000). However, its applicability has not been validated sufficiently through comparison with experimental results.

Visualization of flow patterns can provide the most direct evidence for validating the flow fields predicted by CFD simulations. The Schlieren method is one of the most convenient and frequently applied optical visualization systems (Merzkirch, 1987). A parallel light passing through a test object is focused by a lens (Schlieren head) in the plane of a knife edge. The light passing through the knife edge is observed by a camera. The gradient of a refractive index, which usually corresponds to the density gradient, in the test object bends the light, and the focal point slightly shifts to the direction that is determined by the direction of the gradient. Accordingly, the observed light intensity increases if the focal point is shifted away from the knife edge, or vice versa. In this way, the refractive index gradient in a test object is visualized as the distribution of light intensity in the observed image.

When the progress of the SCWO of a carbon particle was analyzed by a CFD simulation, taking into account the surface reaction of the particle and its enthalpy change, it was suggested that the temperature of the particle was increased by the heat of surface reaction and its relatively high temperature induced an upward flow of supercritical water from the particle, that is, buoyancy-driven flow. A shadowgraph observation of the reaction progress, using a high-pressure cell equipped with transparent windows, sometimes provided images that suggested the existence of such buoyancy-driven flow. When we observe a flame in ambient atmosphere using the Schlieren method, the density gradient around the flame can be clearly visualized. The density gradient around a particle during SCWO is calculated to be much larger than that around a flame in ambient atmosphere. Therefore, by observing the progress of SCWO of a carbon particle using the Schlieren method, it will be possible to visualize the density gradient around the particle, and thus to validate the results of a CFD simulation.

In this work, we observed the progress of SCWO of a carbon particle ($\sim$ 3.5 mm in diameter) using the Schlieren method. Converting Schlieren images to the flow field around the particle was not straightforward because the brightness distribution of the image depended on the "gradient" of the density field and, furthermore, the three-dimensional (3-D) gradient around the particle resulted in two-dimensional (2-D) images that we observed. Therefore, we analyzed the problem the other way around. We simulated the flow field around the particle by CFD simulations. Then, the density field around the particle obtained by the simulation was numerically converted to Schlieren images. By comparing observed and simulated Schlieren images, we were able to confirm that a buoyancy-driven upward flow around a particle actually existed in the SCWO of a carbon particle.

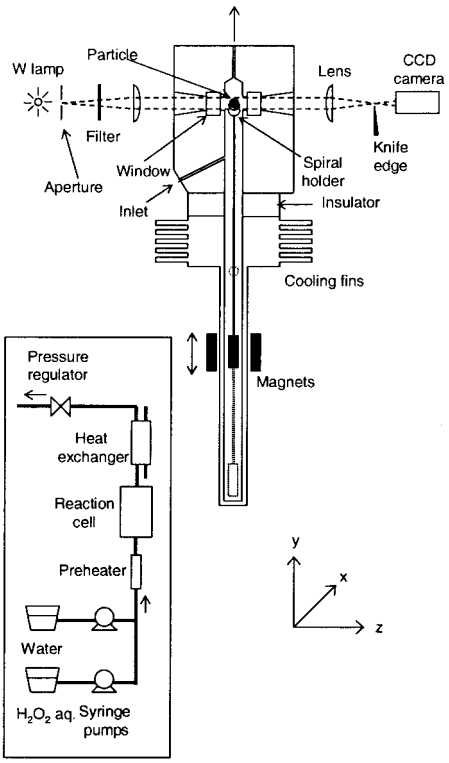

Figure 1. Experimental setup for observing Schlieren image of the supercritical water around a carbon particle.

A carbon particle was attached to the transfer rod with the spiral platinum wire. It was initially held in the cylinder under the cooling fins and then transferred to the center of the cell after an experimental condition was stabilized. Dotted lines indicate the optical path for observing Schlieren images. The origin of the Cartesian coordinate is the center of the particle. The flow diagram is shown in the panel.

Experimental and Numerical Methods

Experimental setup

The experimental setup is shown in Figure 1, which consists of the reaction cell, the flow systems, and the optical setup for observing Schlieren images. The cell consisted of a Hastelloy block with a sample-transfer mechanism. Inside of the cell was the vertical cylinder (8 mm in diameter), with the cross equipped with four sapphire windows at the position where the particle was observed. The cell was controlled to be at supercritical temperatures using four rod heaters and a thermocouple embedded in the Hastelloy block. The cell was connected to the other cylinder through a ceramic insulator and the cooling fins, because of which the temperature of the lower cylinder is kept below 373 K. The particle was clamped to a Hastelloy rod (1.6 mm in diameter) using a platinum wire. The other end of the rod was attached to a magnet. The magnet was coupled with the other magnet outside of the cell for moving the rod. The distance between the fluid inlet and the center of the cell, where the particle was observed, was 40 mm. The flow exited upward.

Two syringe pumps (Isco 100DM) supplied water and an

aqueous solution of H_2O_2, respectively. H_2O_2 was completely decomposed to O_2 and H_2O and stoichiometrically in the preheater (Croiset, 1997), the temperature of which was the same as that of the hot zone of the cell. Therefore, the O_2 fraction in the supercritical fluid can be calculated from the H_2O_2 concentration in the syringe pump, assuming its complete and stoichiometric decomposition. The outlet of the preheater discharged into the cell through the Hastelloy tube (1.6 mm in diameter and about 200 mm in length) surrounded by glass wool, and the temperature of the fluid at the inlet of the cell should be somewhat lower than that of the cell. The fluid was introduced to the cylinder through the narrow inlet (1 mm in diameter). The pressure inside of the cell was controlled by the backpressure regulator (Jasco SCF-Bpg).

The optical setup consisted of the tungsten lamp, the aperture (1 mm in diameter), the green filter to avoid chromatic aberration, two convex lenses, and the knife edge (Mizojiri Optical Co., Ltd.). The focal length of the lenses was 50 mm. A parallel light passing through the cell was focused on the knife edge, as shown in Figure 1. Schlieren images were then formed on a CCD camera, which was continuously recorded on a video tape. Frames of Schlieren images were recorded every 1/30 s.

Two kinds of carbon particles were used: activated carbon and synthetic graphite. Both particles were nearly spherical with a diameter of about 3.5 mm. The density of the activated carbon was 0.75 g cm^{-3}, and the Brunauer–Emmett–Teller (BET) specific surface area was 1.0×10^3 m^2 g^{-1}. The characteristic size of the pore diameter was approximately 5Å. The density of the synthetic graphite was 1.8 g cm^{-3}, and the BET specific surface area was 0.78 m^2 g^{-1}.

The experimental procedure was as follows. While stabilizing a reaction condition in the cell, the particle was kept in the lower cylinder. Then, the particle was transferred into the cell. It took several seconds to transfer the particle and to fix it to the center of the cell. The experimental conditions were as follows: the total pressure was 25 MPa, the temperature of the Hastelloy block was 723 K, the total flow rate at normal temperature and pressure was 0.5 cm^3 min^{-1}, and the O_2 concentration was 3.6 wt %, if added.

CFD simulation

To simulate the flow field and the transfer of heat and mass, we executed CFD calculations with FLUENT version 6 (Fluent Inc.). The simulation corresponds to the SCWO of an activated carbon particle. In the grid imitating the reactor geometry, the particle was modeled as a sphere of 3 mm in diameter, and the rod (1.6 mm in diameter) was directly connected to the particle without modeling the platinum wire surrounding the particle. The grid consisted of 49,361 hexagonal and tetragonal meshes. For simulating the mass transport around the particle, the meshes were densely divided in the vicinity of the particle surface.

Because the Reynolds number near the fluid inlet exceeded 10,000 because of its small diameter (1 mm), a k–ε model for turbulent flow was used. Because the Grashof number was approximately 10^8, the effect of buoyancy was also taken into account in the simulation. This was done by assuming temperature-dependent density of the fluid and gravitational force.

The values of density, specific heat, viscosity, and thermal conductivity were input as piecewise functions of temperature. The properties of the mixture fluid, which consisted mainly of H_2O, O_2, and CO_2, were approximated by the values of pure water (Lemmon et al., 2003; Sengers, 1986). The pressure dependency of fluid properties was neglected because the variation of pressure appears negligible compared to the temperature distribution, especially when the heat of surface reaction at the particle was significant. The temperature at the inner wall of the cell was fixed to be the temperature of the Hastelloy block, and the heat flux from the particle surface to the center of the particle was set to be zero, providing that the particle was thermally in a steady state. The temperature of the fluid at the inlet was not measured but was tentatively set to be 573 K. This value had little effect on the simulated flow field around the particle so long as the value was lower than the wall temperature.

The overall surface reaction of carbon oxidation was modeled as $C + O_2 \rightarrow CO_2$ ($\Delta H = -383$ kJ mol^{-1} at 723 K). The reaction rate was assumed to be first order with respect to O_2 concentration, and the reaction probability of O_2 at the surface was set to be unity. This assumption led to mass transfer–limited kinetics, corresponding to the experiments of the activated carbon particles (Sugiyama et al., 2002). The binary diffusion coefficient of O_2 in supercritical water was approximated by the self-diffusion coefficient of supercritical water (Lamb et al., 1981) because reliable data for the binary diffusion coefficient were not available at this stage.

Numerical method for simulating Schlieren images

Let us consider the Cartesian coordinate in which the z-axis is oriented to the direction of light propagation, and the x- and y-axes are horizontal and vertical direction in a Schlieren image, respectively, as shown at the bottom of Figure 1. The light propagating through a fluid is bent as a result of the gradient of its refractive index. At a given point (x, y, z) in the fluid, the light is bent by the angle $d\theta_x$ from the z coordinate to the direction of x-axis, while it propagates the distance dz attributed to the gradient of refractive index n in the x direction (Merzkirch, 1987)

$$d\theta_x = \frac{1}{n}\frac{\partial n}{\partial x}\,dz \tag{1}$$

This infinitesimal angle $d\theta_x$ accumulates to the angle $\theta_x(x, y)$ while the light passes through the fluid

$$\theta_x(x, y) = \int_{z1}^{z_2} \frac{1}{n}\frac{\partial n}{\partial x}\,dz \tag{2}$$

where z_1 and z_2 correspond to the boundary of the region in which the gradient of refractive index is formed. In the present work, the region is inside of the cell. When the knife edge is inserted perpendicular to the x-axis to the center of the focal spot that is formed by the second convex lens, half of the beam is screened by the knife edge when $\theta_x = 0$. If the beam is bent because of the gradient of refractive index, the focal spot is shifted to the x direction by

$$\Delta h_x(x, y) = \theta_x(x, y) \times f \tag{3}$$

where f is the focal length of the second convex lens (50 mm). Given that $\Delta h_x(x, y)$ is sufficiently smaller than f, the light passing through the focal point reaches the point (x', y') at the surface of the CCD, regardless of the value of $\Delta h_x(x, y)$. The point (x', y') in the observed image corresponds to the position (x, y) in the fluid, and the information on the density gradient of the fluid in the z direction is integrated at each (x, y) position, as expressed in Eq. 2.

In the present calculation, the focal spot is assumed to be spherical with the diameter R (0.5 mm, the same value as the aperture), and the light intensity $I(x, y)$ is obtained by the extent to which the focal spot is screened by the knife edge, which is determined by $\Delta h_x(x, y)$

$$I(x, y) = \frac{2}{\pi R^2} \int_{\Delta h_x(x,y)}^{R} \sqrt{R^2 - a^2}\, da \tag{4}$$

where we assumed that the knife edge is inserted from the $+x$ direction. $I = 1$ corresponds to the intensity when no knife edge is inserted.

A Schlieren image is simulated by calculating $I(x, y)$, which necessitates the value of $n(x, y, z)$. The value of n was related to the density ρ using a linear relation based on the formula suggested by Harvey et al. (1998). The value of $\rho(x, y, z)$ was obtained by the CFD simulation as described above. Calculated values of $I(x, y)$ were converted to a bitmap image and were compared with the Schlieren image obtained by experiments.

This method was validated by observing the Schlieren images of a simple one-dimensional (1-D) linear temperature gradient, which was formed in water at atmospheric pressure between two heated plates. The detail of this validation is described in the Appendix.

Results and Discussion

Schlieren images

Schlieren images obtained for three different conditions are shown in Figure 2. Figure 2a is an activated carbon particle in supercritical water without oxygen, Figure 2b is an activated carbon particle in supercritical water containing oxygen, and Figure 2c is a synthetic graphite particle in supercritical water containing oxygen. For the particles in the Figures 2a and 2c, no decrease in size was observed. On the other hand, the particle in Figure 2b gradually decreased in size and finally vanished within about 900 s. These trends are consistent with the following observations: (1) the rate of size decrease of the activated carbon was almost proportional to the oxygen concentration and no size decrease was observed without oxygen; (2) the rate of size decrease for the activated carbon was about two orders of magnitude larger than that for the synthetic graphite at 723 K. Therefore, it is concluded that substantial oxidation of the particle proceeded only in the condition of Figure 2b.

Correspondingly, a significant contrast was observed above and around the particle only in Figure 2b. This contrast was observed as soon as the particle came into view. It disappeared when the particle vanished. This trend suggests that an upward flow existed during oxidation of the particle. This is consistent with the fact that no contrast was observed in Figures 2a and c, in which no oxidation of particle appeared to proceed. The oxidation of the activated carbon particle appears to have started during the sample

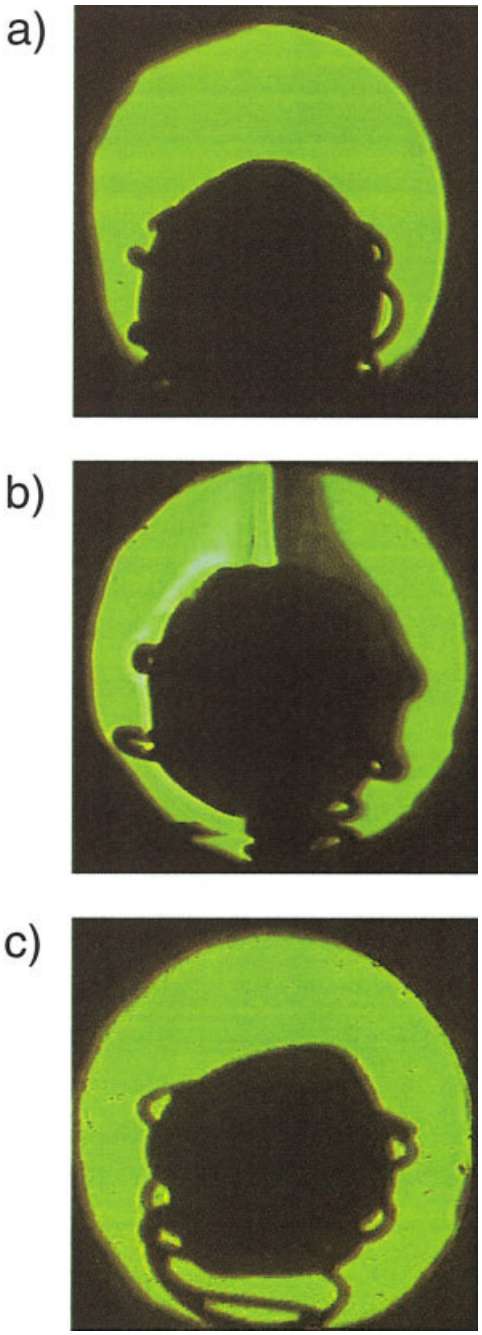

Figure 2. Schlieren images of carbon particles in supercritical water.

(a) An activated carbon in supercritical water without oxygen; (b) an activated carbon in supercritical water containing oxygen; (c) a synthetic graphite in supercritical water containing oxygen. No decrease in the size of the synthetic graphite was observed while the activated carbon vanished by oxidation within about 900 s. Outer circles represent the edge of the windows, which appear to be distorted because of insulating jackets around the cell. The inner shadow is the particle. Spiral support of a platinum wire is seen around the particle. Only for condition (b), the contrast corresponding to the density gradient is seen around and above the particle.

transfer, and thus the temperature of the particle appears to have followed the temperature of the surrounding fluid within an order of seconds.

Although the image is a snapshot of continuously recorded images, the contrast shown in Figure 2b was steady. No apparent difference was observed between successive frames taken every 1/30 s, nor did we admit any change in a time scale of several seconds. When the particle was moved to adjust its position at the initial stage of the experiment, the contrast was distorted according to the change in the flow field, but it stabilized within a second. The width of the contrast above the particle decreased in width as the particle size decreased with oxidation time in a time scale of minutes. It is probable that the contrast was caused by oxidation of the particle and did not reflect inherent fluctuation of the density of supercritical water.

CFD simulation

To obtain a hint as to what is occurring in the cell, CFD simulations were executed. Figure 3 shows (a) path lines that are the tracks of the virtual particles having no weight, (b) temperature distribution, and (c) density distribution on the $z = 0$ plane inside the cell. The origin of the coordinate is the center of the particle. The surface temperature of the particle was higher than that of the surroundings because of the heat of surface reaction ($C + O_2 \rightarrow CO_2$, $\Delta H = -383$ kJ mol^{-1} at 723 K). The heat cannot conduct inside the particle because of the adiabatic boundary condition, which corresponds to a steady state. The heat was dissipated to the surrounding fluid, which flowed out of the cell with the fluid. As a result, the temperature profile as shown in Figure 3b was formed. Accordingly, the distribution of fluid density was formed as shown in Figure 3c. In this simulation, the density distribution was caused solely by the temperature-dependent density of water, and no effect of coexisting O_2 and CO_2 was taken into account. Such effect of composition on fluid density appears negligible compared to the effect of temperature. According to the equation of state by Heilig and Frank (CSOF/SWPA EOS) (Heilig et al., 1989) and using the parameters for the water–N_2 mixtures (because of the lack of those for water–O_2 mixtures), the existence of 3.6 wt % O_2 in water reduces the fluid density by 3.2%, which is smaller than the density variation by approximately 100% shown in Figure 3c.

This density gradient caused two characteristic flow patterns, as shown in Figure 3a. Around the lower part of the particle, the fluid flows to the particle surface. Around the upper part of the particle and above the particle, there was a strong upward flow, caused by buoyancy. The velocity magnitude below the particle was much smaller than that around the particle and the flow direction appeared random.

The simulation assumed a steady state. The flow pattern around and above the particle was stable regardless of the method of convergence. On the other hand, the flow pattern below the particle obtained by the simulation was dependent on the method of convergence, although the trend of randomly oriented flow vector with relatively small velocity magnitude was invariant. This is because the flow below the particle was unstable because of the lack of its driving force.

The only driving force for flow in the cell appears to be the higher temperature of the particle. The large inlet velocity resulting from the narrow inlet can be another driving force for flow, but the lower temperature of the inlet prevented the fluid from moving upward because of buoyancy effect. Considering that the reaction rate of the activated carbon particle was limited by external mass transfer of O_2, such flow around the particle, caused by the heat of surface reaction, should have enhanced mass transfer and thus have accelerated the reaction, leading to a kind of positive feedback. Therefore, simulating

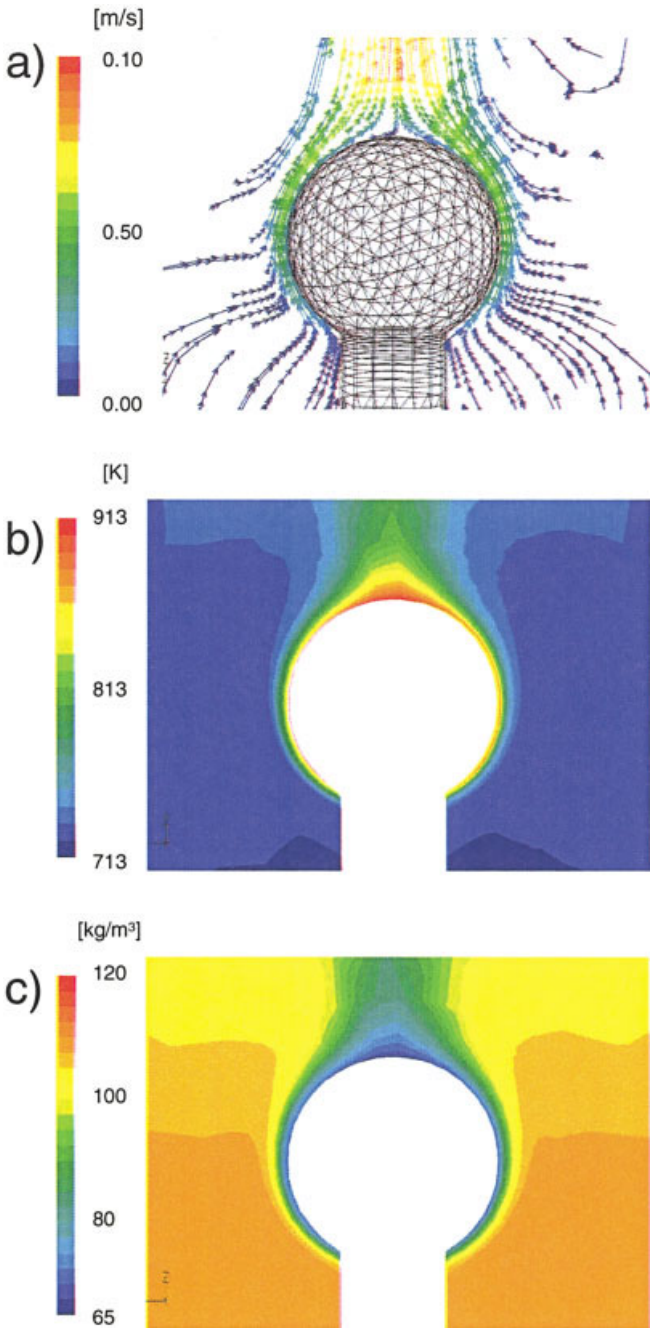

Figure 3. Results of CFD simulations of supercritical water containing oxygen around a particle of activated carbon and its supporting shaft.

(a) Path lines colored by velocity magnitude, (b) temperature contour, and (c) density contour. The surface reaction of oxygen with the particle and its enthalpy change were taken into account.

flow patterns caused by the heat of surface reaction is essential for accurate prediction of the rate of SCWO of solid substances.

Simulated Schlieren image

To validate the flow patterns obtained by the CFD simulations using Schlieren images obtained by experiments, it is necessary to convert a 3-D distribution of density around the particle to a 2-D Schlieren image. The method is described in the previous section.

The Schlieren image thus obtained is shown in Figure 4. Qualitatively, the simulated image agreed well with the observed image in Figure 2b. Therefore, it is certain that the upward flow caused by the heat of surface reaction actually existed, and this flow pattern was able to be predicted by CFD simulations.

To compare the experimental and numerical Schlieren images quantitatively, the variation of the brightness on the horizontal line in the x direction at 2 mm above the center of the particle was observed, as shown by the solid line in Figure 5. The maximum brightness of unity corresponds to the value when no knife edge was inserted into the optical path. With respect to the bright part of the image (left side), agreement between the experimental result and simulation was good. However, for the dark part (right side), simulation appears to overestimate both darkness and width of the dark region. It is possible that the density gradient was overestimated in the CFD simulation with the surface reaction of $C + O_2 \rightarrow CO_2$.

A possible cause of this overestimation is that the surface reaction assumed in the simulation was wrong. Therefore, another simulation was executed assuming an alternative surface reaction: $2C + O_2 \rightarrow 2CO$ ($\Delta H = -201$ kJ mol^{-1} at 723 K). For this reaction, heat released by one mole of O_2 was smaller than that of the original reaction. We compared the heat by one mole of O_2 because the reaction rate was limited by external mass transfer of O_2 to the particle. A smaller amount of heat released by the surface reaction led to the lower temperature of the particle: the simulated temperature averaged on the particle surface was 777 K with this alternative reaction, whereas it was 885 K with the original reaction. As a result, simulated brightness in Figure 5 is closer to the experimental result. This alone cannot lead to the conclusion that the surface reaction occurring in the course of the SCWO of an activated carbon particle is $2C + O_2 \rightarrow 2CO$, but the present result suggested its possibility.

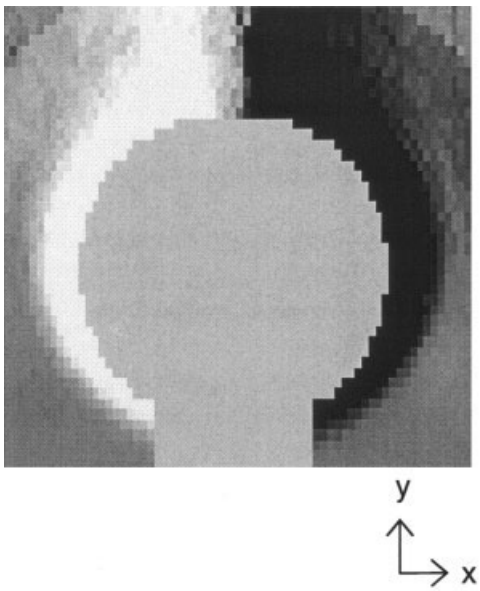

Figure 4. Schlieren image predicted from a 3-D density distribution obtained by CFD simulation.

The circle at the center is the image of an activated carbon particle. The rectangle below the circle is the image of the supporting rod.

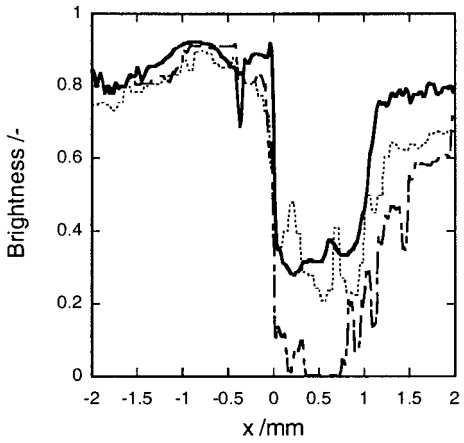

Figure 5. Variation of the brightness along the horizontal line at 2 mm above the center of the particle.

The position $x = 0$ corresponds to the center of the particle. The solid line is the experimental result and the dashed line is for the result of the simulation, assuming the surface reaction of $C + O_2 \rightarrow CO_2$ ($\Delta H = -383$ kJ mol^{-1} at 723 K). The dotted line is the simulated contrast, assuming the surface reaction of $2C + O_2 \rightarrow 2CO$ ($\Delta H = -201$ kJ mol^{-1} at 723 K).

Conclusions

The flow field in the SCWO of carbon particles was analyzed by a combined approach of flow visualization and CFD simulation. By the use of Schlieren optics, the density distribution around the particle was successfully visualized. The Schlieren image of the flow around the activated carbon particle was in good qualitative agreement with a simulated Schieren image. Moreover, in a comparison of the light intensity along a horizontal line, there was good quantitative agreement, at least for the bright side of the image. It was confirmed that a CFD simulation with appropriate assumptions can predict flow patterns in SCWO of solid substances.

It was also revealed that the heat of reaction increases the temperature of solid substances and thus induces a buoyancy-driven flow around them, leading to positive feedback of their reaction rate when the external mass transfer of oxygen is the limiting step. Therefore, predicting flow fields in SCWO reactors is of crucial importance and is possible by CFD simulations.

Acknowledgments

The present study was supported in part by a grant provided by the New Energy and Industrial Technology Development Organization [NEDO, via

Japan Chemical Innovation Institute (JCII)] based on the project "Research & Development of Environmentally Friendly Technology Using SCF" of the Industrial Science Technology Frontier Program [Ministry of Economy, Trade and Industry (METI), Japan], which is greatly appreciated.

Literature Cited

Croiset, E., S. F. Rice, and R. G. Hanush, "Hydrogen Peroxide Decomposition in Supercritical Water," *AIChE J.*, **43**, 2343 (1997).

Fluent Inc., Lebanon, NH, http://www.fluent.com/.

Harvey, A. H., J. S. Gallagher, and J. M. H. L. Sengers, "Revised Formulation for the Refractive Index of Water and Steam as a Function of Wavelength, Temperature and Density," *J. Phys. Chem. Ref. Data*, **27**, 761 (1998).

Heilig, M., and E. U. Franck, "Calculation of Thermodynamic Properties of Binary Fluid Mixtures to High Temperatures and High Pressures," *Ber. Bunsenges. Phys. Chem.*, **93**, 898 (1989).

Lamb, W. J., G. A. Hofmann, and J. Jones, "Self-Diffusion in Compressed Supercritical Water," *J. Chem. Phys.*, **74**, 6875 (1981).

Lemmon, E. W., M. O. McLinden, and D. G. Friend, "Thermophysical Properties of Fluid Systems in NIST Chemistry WebBook," P. J. Linstrom, and W. G. Mallard, eds., National Institute of Standards and Technology, Gaithersburg, MD 20899 (http://webbook.nist.gov) (2003).

Merzkirch, W. *Flow Visualization*, 2nd ed., Academic Press, Orlando, FL (1987).

Oh, C. H., R. J. Kochan, T. R. Charlton, and A. L. Bourhis, "Modelling of Thermal Characteristics in Supercritical Water Oxidation Reactors," Proc. of 1995 ASME International Mechanical Engineering Congress and Exposition. Part 2, American Society of Mechanical Engineers, San Francisco, CA, November 1995, ASME Heat Transfer Division Publication HTD v 317-2, pp. 311–320 (1995).

Savage, P. E., "Organic Chemical Reactions in Supercritical Water," *Chem. Rev.* **99**, 603 (1999).

Scion Corp., 82 Worman's Mill Court, Suite H, Frederick, MD 21701.

Sengers, J. V., and J. T. R. Watson, "Improved International Formulations for the Viscosity and Thermal Conductivity of Water Substance," *J. Phys. Ref. Data*, **15**, 1291 (1986).

Sugiyama, M., H. Ohmura, M. Kataoka, T. Kobayashi, and S. Koda, "Shadowgraph Observation of Supercritical Water Oxidation Progress of a Carbon Particle," *Ind. Eng. Chem. Res.*, **41**, 3044 (2002).

Tester, J. W., H. R. Holgate, F. J. Armellini, P. A. Webley, W. R. Killilea, G. T. Hong, and H. E. Barner, "A Review of Process Development and Fundamental Research," ACS Symposium Series 518, Chapter 3, American Chemical Society, Washington, DC (1993).

Zhou, N., A. Krishnan, F. Vogel, and W. A. Peters, "A Computational Model for Supercritical Water Oxidation of Organic Toxic Wastes," *Adv. Environ. Res.*, **4**, 79 (2000).

Appendix: Validation of the Method for Estimating Schlieren Images

To validate the numerical method for obtaining Schlieren images, it is effective to observe the Schlieren images formed by the uniform 1-D gradient of a refractive index. In this case, Eq. 2 is calculated analytically and we can avoid errors stemming from numerical processing. The 1-D gradient of the refractive index can be formed by the temperature gradient between two parallel plates with different temperatures, as shown in Figure A1a. In this setup, water is used to fill the glass vessel (height 26 mm, width 70 mm in the direction of light propagation). The density gradient of water was formed in the y direction by the temperature difference, which formed a Schlieren image. The size of heated plates was larger than the width of the glass vessel, to avoid a fluctuation of temperature gradient near the edges of the plates. The temperature of the upper plate was greater than that of the bottom plate to avoid buoyancy-driven flows. The temperature of the bottom plate was fixed to 35°C and the temperature of the upper heater was varied from 35 to 80°C. For each temperature, a Schlieren image was observed after the stabilization of the temperature gradient. The knife edge was inserted from the $+y$ direction to the center of the optical path.

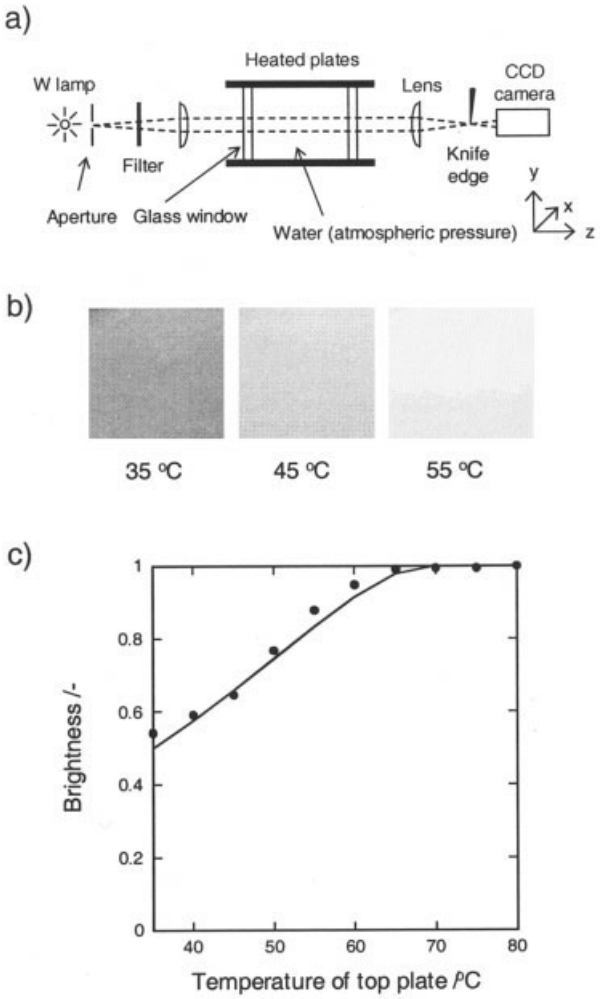

Figure A1. (a) Experimental setup for observing Schlieren images of a 1-D linear temperature gradient formed in water between two parallel plates.

The temperature of the upper plate was higher than that of the lower plate. The knife edge was inserted from the upper side. (b) Observed Schlieren images for the upper plate temperatures of 35, 45, and 55°C while the temperature of the bottom plate was fixed to 35°C. (c) Brightness of the Schlieren images (circles) as a function of temperature of the upper plate while temperature of the bottom plate was fixed to 35°C. The solid line indicates the estimated brightness based on the method used in this work.

The observed Schlieren image had uniform light intensity in the whole plane, as shown in Figure A1b, indicating that the temperature gradient in the glass vessel was indeed uniform. As the temperature of the upper plate increased, the brightness of the image increased. This change in brightness was digitized using Scion Image software (Scion Corp.). The brightness was plotted as shown in Figure A1c.

The maximum brightness of unity corresponds to the value when no knife edge was inserted into the optical path. Qualitatively, this is because the higher temperature of the upper part of the water column decreased its refractive index and thus bent light to the $-y$ direction, opposite to that of the knife edge. For quantitative analysis, the brightness of Schlieren images was calculated using Eqs. 2–4, as plotted by the solid line in Figure A1c. Agreement with the experimental data is excellent, indicating that the method for estimating Schlieren images is valid.

Manuscript received Aug. 20, 2003, and revision received Jan. 6, 2004.